Biophysical Chemistry 26 (1987) 279–290
Elsevier

BPC 01145

Structure of halophilic malate dehydrogenase in multimolar KCl solutions from neutron scattering and ultracentrifugation

Patrick Calmettes [a], Henryk Eisenberg [b] and Giuseppe Zaccai [c]

[a] *Laboratoire Léon Brillouin, CEN Saclay, 91191 Gif-sur-Yvette Cedex, France,*
[b] *Polymer Department, The Weizmann Institute of Science, Rehovot 76100, Israel*
and [c] *Institut Laue-Langevin, 156X, 38042 Grenoble Cedex, France*

Accepted 27 February 1987

Halophilic enzyme; Halobacteria; Malate dehydrogenase; Neutron scattering; Ultracentrifugation; Enzyme structure

The structure and solvent interactions of malate dehydrogenase from *Halobacterium marismortui* in multimolar KCl solvents are found to be similar to those in multimolar NaCl solvents reported previously (G. Zaccai, E. Wachtel and H. Eisenberg, J. Mol. Biol. 190 (1986) 97). KCl rather than NaCl is predominant in physiological medium. At salt concentrations up to about 3.0 M, the protein (a dimer of M 87000 g/mol) can be considered to occupy an invariant volume in which it is associated with about 4100 molecules of water and about 520 molecules of salt. At very low resolution, the enzyme particle appears to have a compact protein core and protruding protein parts in interaction with the water and salt components, structural features that are not observed in non-halophilic mitochondrial malate dehydrogenase. The above conclusions were drawn from the analysis of neutron scattering and ultracentrifugation data, and the complementarity of these approaches is discussed extensively.

1. Introduction

The survival of both higher and lower organisms is strongly linked to the environment and the disappearance of widespread forms of life in the history of our planet may have been due to sudden changes in the environment. Gradual changes, however, could permit both lower and higher forms of life to adapt to modifications in temperature, salinity, acidity, pressure, humidity and elemental composition of the surrounding medium. It has thus become a problem of considerable interest to explore the limits of biological adaptation to extreme conditions, including those evolutionary aspects which lead to phenotypic and genotypic modifications. Though 'normal' life today proceeds in what we would characterize as a temperate environment, numerous examples of life in extreme environments have recently come to the fore.

The biological machinery of the extreme halophilic bacteria functions at concentrations of salt at which proteins in non-halophilic cells would be salted out and cease to function. Salt requirements differ, but concentrations can be extremely high inside these cells. Certain halophilic bacteria are equipped with K^+ pumps such that the intracellular KCl concentration exceeds the exterior concentration of the medium manyfold, as well as substantially exceeding the solubility limit of this electrolyte in water. A mechanism of active chloride accumulation in *Halobacterium halobium* has been associated with halorhodopsin, a retinal protein found in the cytoplasmic membrane [1]. Considering this and the fact that the most distinctive compositional feature differentiating between halophilic and non-halophilic proteins is a conservative increase in acidic over basic amino acids [2], it becomes clear that a deeper knowledge of protein structure is essential to understanding

We dedicate this work to the happy occasion of the 60th birthday of Professor Manfred Eigen, a great scientist and friend.

Correspondence address: G. Zaccai, Institut Laue-Langevin, 156X, 38042 Grenoble Cedex, France.

halophilic stability and function. Five years ago Jaenicke [3] extensively reviewed the behavior of enzymes under extremes of physical conditions. The present work aims at contributing towards a better understanding of structural aspects in the extreme halophile bacteria.

The halobacteria have been classified as belonging to the archaebacteria, one of the three main branches in the unrooted evolutionary tree. The other two are the better known eubacteria (also named prokaryotes) and eukaryotes [4]. A recent and extensive review on the archaebacteria [5] discusses their biochemical diversity and ecology, translation apparatus and general molecular characteristics, by considering cell envelopes, lipids and genome structure. Kushner [6] reviews the Halobacteriaceae including characterization of a variety of salt habitats, halophilic and halotolerant microorganisms, definition and classification of the *Halobacterium* and *Halococcus* species (family Halobacteriaceae) as well as a summary of the halobacteria of the Dead Sea identified with the original *H. marismortui* [7]. The halophilic malate dehydrogenase (hMDHase) whose properties are discussed in this work, was purified from the so-called Ginzburg isolate [6,8] believed to correspond to the lost original *H. marismortui* strain.

The interactions of a biological macromolecule must proceed through its environment, and understanding the structure and influence of this environment might be as important for the understanding of function as the knowledge of the macromolecular structure which, of course, is itself strongly correlated with solvent effects. Interactions between biological molecules and solvent components can be studied by the usual physicochemical techniques, including scattering methods. It has been shown that in the thermodynamic limit the information derived from forward scattering depends on a density increment similar to that measured in sedimentation experiments except for the substitution of the mass of the components by their appropriate scattering lengths [9,19]. Small-angle X-ray scattering (SAXS) experiments, for example, yield thermodynamic information which is similar to that given by sedimentation or densitometric investigations because X-rays are scattered by electrons and electron densities are nearly proportional to mass densities. Neutron scattering length densities, on the other hand, are completely uncorrelated with mass densities so that small-angle neutron scattering (SANS) experiments provide complementary data to those from SAXS or densitometric studies. This approach has been used recently in conjunction with sedimentation and SAXS experiments carried out on hMDHase in solutions containing different concentrations of NaCl [10]. The interactions of halophilic proteins with solvent components appear to be very different from those of non-halophilic proteins. In NaCl solvents, for example, it was found that hMDHase associates unusually high amounts of water and NaCl [10–12]. As the natural environment of hMDHase contains a very high concentration of KCl rather than NaCl [8], it was appropriate to extend this work to a study of the enzyme and its solvent interactions in KCl solutions. We find that the unusual solvent interaction properties documented in NaCl solutions are maintained in KCl. The concept of an invariant macromolecular particle is also discussed in this paper insofar as it can be deduced from experimental data.

A low-resolution structure of both hMDHase and its microenvironment is proposed and compared with that of a non-halophilic mitochondrial malate dehydrogenase.

2. Materials and methods

2.1. Materials

hMDHase from *H. marismortui* was purified as described previously [12]. All buffers contained KCl at the appropriate concentration and 50 mM potassium phosphates adjusted to pH 7. hMDHase concentrations were determined by ultraviolet absorption using $A^{0.1\%}_{280\,nm} = 0.802$ cm^2 mg^{-1} [13].

For SANS experiments, a stock solution of the enzyme was first prepared by dialysis against the buffer with the highest KCl concentration used, namely, 3.8 M. For this stock solution the concentration of hMDHase was 10 mg/ml. Different hMDHase samples of various KCl concentrations were obtained by dilution. Control solutions of buffer alone were simultaneously prepared using

the same pipette settings. A similar procedure was used for sedimentation measurements for KCl concentrations lower than 2.0 M. For higher concentrations hMDHase samples were obtained by dialysis against suitable solvents. For such KCl concentrations hMDHase does not denature [11].

Solutions of mitochondrial malate dehydrogenase (mMDHase) from pig heart in 50% (v/v) glycerol in water were obtained from different manufacturers. Almost all samples showed a tendency to aggregate and to form a deposit in the containers. This trend increased with increasing temperature. The most stable mMDHase solution was from Boehringer, Mannheim, and was therefore chosen for the experiments. mMDHase sample solutions were prepared in the cold (4° C). Commercial solutions were first dialysed against the appropriate KCl buffer at pH 7.0. Aggregates were removed by centrifugation. The samples were then concentrated to about 1.0% with Centricon-10 micro-concentrators. Concentrations were measured by ultraviolet absorption using $A^{0.1\%}_{280\ nm} = 0.390\ cm^2\ mg^{-1}$ (this value was made known to us by one manufacturer, Biogenzia Lemania, S.A., Switzerland). As soon as possible after preparation, neutron scattering measurements were carried out at 4.0 ± 0.5° C. In all cases, aggregates appeared 2–3 days after preparation so that an extensive neutron scattering study of mMDHase in solution is rather difficult.

2.2. Neutron scattering

For hMDHase, all neutron scattering data were collected at room temperature using fused silica spectrophotometer cuvettes of 1.00 mm path length. Similar cuvettes were also employed for solutions of mMDHase in light water, but 2.00 mm path length cuvettes were used with heavy water (^2H_2O). SANS experiments on hMDHase in light water buffers were performed on the D11 instrument at the Institut Laue-Langevin, Grenoble [14]. The sample-to-detector distance D was 2.60 m and the neutron wavelength, λ, was either 10.0 or 4.48 Å, giving respective wave number transfers q ranging either from 1.3×10^{-2} to 9.0×10^{-2} Å^{-1} or from 2.2×10^{-2} to 1.9×10^{-1} Å^{-1}. The irradiated volume was about 0.1 ml. All other SANS experiments were carried out on the PACE spectrometer at the Laboratoire Léon Brillouin, Saclay [15]. SANS from mMDHase solutions were recorded for 6.5×10^{-3} Å$^{-1} < q < 6.8 \times 10^{-2}$ Å^{-1} with $\lambda = 10.4$ Å and $D = 2.80$ m. hMDHase and mMDHase were also studied at larger wave numbers ranging from 4.7×10^{-2} to 4.7×10^{-1} Å^{-1}. In this case ^2H_2O buffers were used in order to reduce incoherent background scattering from the solvent. Intensities recorded at different angles were corrected for uniformity of detector response by normalization to the incoherent scattering of a water sample. By calibrating this water sample, scattered intensities were placed on an absolute scale [16]. The background scattering due to the solvent alone was subtracted. Because the incoherent scattering from the solutes is different from that of the solvents (this is especially true for deuterated solvents) this method is not sufficiently accurate for correcting the low intensities recorded at the larger q values. Consequently, background subtraction in these cases was made in such a way that the remaining scattered intensity vanishes on average in the range 3.3×10^{-1} Å$^{-1} < q < 4.7 \times 10^{-1}$ Å^{-1}.

When processed as explained, SANS measurements give the q-dependent absolute value of the coherent intensity, $I(q)$ scattered by the sample. The thermodynamic limit $I(0)$ is obtained from $I(q)$ at small q by using the Guinier approximation [17]:

$$I(q) = I(0)\ \exp\left(-q^2 R_g^2/3\right) \tag{1}$$

where R_g is the radius of gyration of contrast within the particle. When the number of particles per unit volume of solution is sufficiently small the forward scattered intensity is given by the expression

$$I(0) = (c_2 M_2/N_A)(\partial \rho_N/\partial c_2)^2_\mu \tag{2}$$

where ρ_N is the scattering length density of the sample solution which is assumed to contain only light or heavy water, protein and salt, referred to as components 1, 2 and 3 respectively. c_2 (g/ml) denotes the concentration of macromolecule and M_2 (g/ml) its molar mass. N_A is Avogadro's number. The subscript μ denotes that the partial de-

rivative is calculated at constant chemical potential of diffusible components (water and salt) and at constant temperature and pressure.

2.3. Sedimentation measurements

Sedimentation experiments were performed at 20°C on a Beckman model E analytical centrifuge. Equilibrium sedimentation measurements were carried out at 15000 rpm for different KCl concentrations varying from 2.0 to 4.0 M. For low hMDHase concentrations the mass density increments were obtained from equilibrium sedimentation by means of the expression [18]

$$(\partial\rho/\partial c_2)_\mu = \frac{RT}{M_2} \cdot \frac{2}{\omega^2} \cdot \frac{\mathrm{d}\ln c_2(r)}{\mathrm{d}r^2} \tag{3}$$

where ρ (g/ml) is the mass density of the sample solution, R the gas constant, ω the angular velocity of the rotor and $c_2(r)$ the enzyme concentration in the centrifuge tube at a level r from the rotor center.

From the measured value $s_{20,sol}$ of the sedimentation coefficient the corrected value $s_{20,w}$ was calculated by means of the expression

$$s_{20,w} = s_{20,sol} \cdot \frac{\eta_{sol}}{\eta_w} \cdot \frac{1-\phi'\rho_w}{1-\phi'\rho^o} \tag{4}$$

where η_{sol} and η_w are the viscosities of the sample and of water and ρ^o and ρ_w the densities of the buffer and of water, respectively. By analogy with simple two-component systems, the quantity ϕ' is defined as follows

$$(\partial\rho/\partial c_2)_\mu = 1 - \phi'\rho^o. \tag{5}$$

2.4. Light scattering

The translational diffusion coefficient $D_{20,sol}$ of the protein particles at 20°C was measured by means of quasielastic light scattering as described previously [12]. The corrected diffusion coefficient $D_{20,w}$ was calculated as follows

$$D_{20,w} = \frac{\eta_{sol}}{\eta_w} \cdot D_{20,sol} \tag{6}$$

For KCl concentrations lower than 2.0 M the density increment was inferred from the experimental values of the diffusion and sedimentation coefficients by means of the Svedberg equation

$$(\partial\rho/\partial c_2)_\mu = \frac{RT}{M_2} \cdot \frac{s_{20,sol}}{D_{20,sol}} \tag{7}$$

From these values the quantity ϕ' was computed according to eq. 5.

3. Theory

3.1. Thermodynamic limit

When a solution of macromolecules in water and salt is in dialysis equilibrium with the water and salt solvent, the mass density increment due to the presence of the macromolecule can be written [9]

$$(\partial\rho^o/\partial c_2)_\mu = 1 + \xi_1 - \rho^o(\bar{v}_2 + \xi_1\bar{v}_1) \tag{8}$$

where ξ_1 is an interaction parameter in g water per g macromolecule, and $\bar{v}_2$ and $\bar{v}_1$ represent the partial specific volumes of the macromolecule and water, respectively. The presence of the macromolecule changes the chemical potential of solvent components in the dialysis bag. To maintain equilibrium with the bath, this change is compensated for by a change in salt concentration. The parameter ξ_1 represents the water required to enter the bag in order to compensate for the disturbance caused to the solvent by the macromolecules. For example, if the macromolecule 'bound' salt, the solvent in the bag would be at an effectively lower salt concentration than that in the bath. To re-establish thermodynamic equilibrium water would have to leave the bag leading to a negative value of ξ_1. Equilibrium could be re-established equally well by an influx of salt instead of an efflux of water, and eq. 8 can be written in terms of ξ_3 and $\bar{v}_3$, with

$$\xi_3/\xi_1 = -w_3 \tag{9}$$

when the solvent contains w_3 g salt per g water. The macromolecule might associate both water and salt, but the solvent composition can be adjusted by either salt or water transfer, so that in general, the value of ξ_1 (or ξ_3) is not the mass of

water (or salt) associated with a gram of macromolecule. There is an equivalent equation to eq. 8 for the neutron scattering length density increment [10,19]

$$(\partial\rho_N/\partial c_2)_\mu = b_2 + \xi_1 b_1 - \rho_N^\circ(\bar{v}_2 + \xi_1\bar{v}_1) \qquad (10)$$

where b_1 and b_2 are the scattering lengths per g water and protein, respectively. Because these values are uncorrelated with the respective mass densities of the components, eqs. 8 and 10 are independent and could be solved for ξ_1 and $\bar{v}_2$ if the other parameters are known. If ξ_1 is linear with w_3^{-1} a model particle might be considered in which the macromolecule is associated with constant amounts of water and salt, B_1 and B_3 g per g macromolecule, respectively, where B_3 includes the Donnan term [10,19].

$$\xi_1 = B_1 - B_3/w_3 \qquad (11)$$

and B_1 and B_3 could be calculated from the straight line's intercept and slope, respectively.

Under these conditions, the density increment can be written:

$$(\partial\rho/\partial c_2)_\mu = 1 + B_1 + B_3 - \rho^\circ(\bar{v}_2 + B_1\bar{v}_1 + B_3\bar{v}_3) \qquad (12)$$

When $(\partial\rho/\partial c_2)_\mu$ is linear with ρ° the model particle made up of the macromolecule and its associated solvent components might be considered to have an invariant volume $V_{tot} = \bar{v}_2 + B_1\bar{v}_1 + B_3\bar{v}_3$ ml per g macromolecule, and a composition of 1 g macromolecule + B_1 g water + B_3 g salt per g macromolecule [10].

For the sake of convenience, in the treatment of the KCl and NaCl data together, eqs. 11 and 12 are re-written in terms of molar quantities.

$$\Gamma_1 = N_1 - N_3(n_1/n_3) \qquad (13)$$

$$(\partial\rho/\partial n_2)_\mu = M_2 + N_1M_1 + N_3M_3 - \rho^\circ(M_2V_{tot}) \qquad (14)$$

Γ_1 is the interaction parameter in mol water per mol macromolecule ($\Gamma_1 = \xi_1 M_2/M_1$; $(\partial\rho/\partial n_2)_\mu = M_2(\partial\rho/\partial c_2)_\mu$), the solution contains n_1 mol/ml water, $n_2 = c_2/M_2$ mol/ml protein and n_3 mol/ml salt; the protein is associated with N_1 ($= M_2B_1/M_1$) mol water per mol and N_3 ($= M_2B_3/M_3$) mol salt per mol; M_1 and M_3 are the molar masses of water and salt, respectively.

These unconvential units have been chosen in order to simplify the equations, and to emphasise that, in the particular case of the interaction parameters, the water and salt components are symmetric. Eq. 13 could be written equally well in terms of the salt interaction parameter:

$$\Gamma_3 = N_3 - N_1(n_3/n_1) \qquad (13a)$$

The relations with conventional notation are the following.

Molarity: C_2 (mol/l) $= 10^3 n_2$ for the macromolecule;
C_3 (mol/l) $= 10^3 n_3$ for the salt.

Molality: m_3 (mol/kg) $= (10^3 n_3)/(n_1 M_1)$ for the salt;
w_3 (g/g) $= m_3 M_3/10^3$.

There is an equivalent equation to eq. 14 for the neutron scattering length density increment [10]

$$(\partial\rho_N/\partial n_2)_\mu = M_2b_2 + N_1M_1b_1 + N_3M_3b_3 - \rho_N^\circ(M_2V_{tot}) \qquad (15)$$

For the same reasons as discussed above for eqs. 8 and 10, eqs. 14 and 15 are independent. If they both defined straight lines, $(\partial\rho/\partial n_2)_\mu$ vs. ρ° and $(\partial\rho_N/\partial n_2)_\mu$ vs. ρ_N°, then the hypothesis of the particle of invariant composition and volume is strengthened. Linearity might occur in one case without this hypothesis being valid, through compensating changes in the parameters, but it is unlikely that it would occur for both the mass and neutron scattering length density increments. In the invariant particle hypothesis, the slopes of the lines should be identical, viz., $M_2V_{tot} = \bar{v}_2M_2 + N_1M_1\bar{v}_1 + N_3M_3\bar{v}_3$, the total volume of the particle per mol protein; the intercepts with the ρ° and ρ_N° axes are $M_{tot} = M_2 + N_1M_1 + N_3M_3$ and $L_{tot} = b_2M_2 + b_1N_1M_1 + b_3N_3M_3$, the total molar mass and molar scattering length of the particle, respectively. These equations could be solved for N_1, N_3 and V_{tot} by putting in the experimental values for the slope and intercepts.

3.2. Particle structure

The coherent intensity of neutrons scattered by a single particle in a solvent is

$$i(q) = \left\langle \left| \int (\rho_N(r) - \rho_N^o) \exp(iq \cdot r \, dr^3) \right|^2 \right\rangle \quad (16)$$

where $\rho_N(r)$ is the local scattering length density in the particle. The wave vector transfer is $q = k_1 - k_0$ where k_1 and k_0 are the respective wave vectors of scattered and incident neutrons. The angular brackets indicate averaging over all orientations of the particle.

For dilute solutions the intensity scattered by all the particles is $\lim_{(c \to 0)} I(q) = c_2 N_A / M_2 \cdot i(q)$. For vanishing values of the wave vector transfer this result is rigorously identical to that given by eq. 2.

Mathematically, it is not possible to obtain $\rho_N(r)$ from eq. 16. Furthermore, different particles may give identical scattering profiles so that experimentally measured $I(q)$ values do not allow a unique model to be selected for representing the data. Nevertheless, certain parameters such as the radius of gyration, R_g, of the particle contrast (eq. 1) can be calculated unambiguously from $I(q)$ [20].

For a two-component particle the parallel axes theorem [21] states that

$$R_g^2 = x_2 R_{g2}^2 + (1 - x_2) R_{gs}^2 + x_2 (1 - x_2) d_{2s}^2 \quad (17)$$

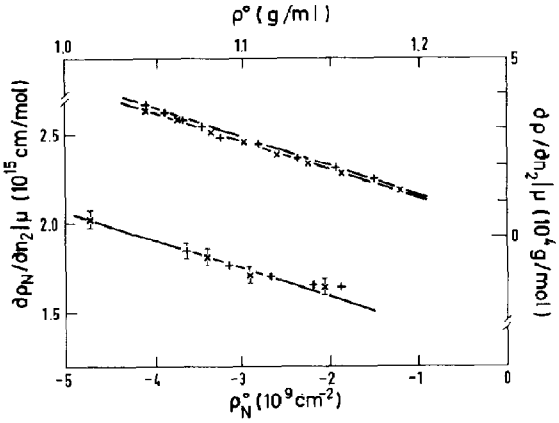

Fig. 1. Scattering length and mass density increments of hMDHase solutions as a function of the scattering length and the mass densities of the interparticle solvent: (+) KCl, (×) NaCl.

where R_{g2} and R_{gs} are the radii of gyration of the macromolecule and of the solvent associated with it, respectively, d_{2s} represents the distance between the centers of excess scattering of the two components and

$$x_2 = \frac{M_2(b_2 - \rho_N^o \bar{v}_2)}{L_{tot} - \rho_N^o V_{tot}} \quad (18)$$

denotes the scattering fraction of the macromolecule.

Table 1

Results from sedimentation and SANS experiments for hMDHase in KCl solutions of concentration C_3

C_3 (mol/l)	n_1/n_3	ρ_N^o (×10⁹) (cm⁻²)	$\left.\frac{\partial \rho_N}{\partial n_2}\right\|_\mu$ (×10¹⁵) (cm/mol)	ρ^o (g/ml)	$\left.\frac{\partial \rho}{\partial n_2}\right\|_\mu$ (×10⁴) (g/mol)	$\bar{v}_2$ (ml/g)	Γ_1 (×10³)
4.00	12.1	−1.70		1.1745	1.633	0.788 [a]	−3.28
3.80	12.8	−1.90	1.636 ± 0.008	1.1658		0.788 [a]	−3.38
3.50	14.1	−2.19	1.656 ± 0.006	1.1529	1.910	0.777 ± 0.004	−3.58
3.00	16.8	−2.68	1.701 ± 0.006	1.1312	2.225	0.767 ± 0.004	−4.46
2.50	20.5	−3.17	1.760 ± 0.010	1.1093	2.615	0.756 ± 0.009	−6.03
2.00	26.0	−3.66	1.842 ± 0.016	1.0875	2.759	0.761 ± 0.015	−8.78
1.75	31.2			1.0765	3.05	0.762 [a]	−11.03
1.50	35.3	−4.15		1.0655	3.25	0.764 [a]	−14.05
1.25	42.7			1.0546	3.46	0.765 [a]	−18.13
1.00	53.8			1.0437	3.70	0.766 [a]	−24.10

[a] Values of $\bar{v}_2$ have been extrapolated according to the continuous curve drawn in fig. 3 and used to calculate the corresponding values of Γ_1 by means of eqs. 8 and 13.

4. Results

4.1. Thermodynamic limit

Values of the scattering length density increments $(\partial\rho_N/\partial n_2)_\mu$ for the different KCl conditions were derived from the Guinier approximation according to eqs. 1 and 2 with $M_2 = 87\,000$ [10]. These are listed in table 1 and plotted in fig. 1 as a function of the scattering length density of the solvent. Only one set of measurements was made and the given uncertainties correspond to one standard deviation. Neglecting the data corresponding to the two higher salt concentrations $(\partial\rho_N/\partial c_2)_\mu$ can be regarded as varying linearly with slope $M_2V_{tot} = (1.5 \pm 0.4/0.2) \times 10^5$ ml per mol protein, and intercept with the $\rho_N^0 = 0$ axis $L_{tot} = (1.29 \pm 0.06/0.12) \times 10^{15}$ cm. For comparison, the data previously obtained for NaCl buffers [10] are also shown in fig. 1. In this case the error bars correspond to different sets of measurements and, therefore, are larger. Within the experimental uncertainties the data points for KCl and NaCl lie on the same curve. For both salts the points at the highest salt concentrations deviate slightly from the straight line. Neglecting the point corresponding to 4.0 M NaCl, the slope of the line is found to be $M_2V_{tot} = (1.5 \pm 0.4/0.2) \times 10^5$ ml per mol protein and its intercept with the $\rho_N^0 = 0$ axis is $L_{tot} = (1.28 \pm 0.06/0.21) \times 10^{15}$ cm, identical values to those of the KCl data.

For equilibrium sedimentation measurements the values of the mass density increments were calculated according to eq. 3 and are given in table 1. It should be noted that, in 2.0 M KCl buffer, hMDHase is not stable [11] so that the value corresponding to this concentration is approximate. The sedimentation and diffusion coefficients of the enzyme were measured for different KCl concentrations ranging from 1.0 to 4.0 M. Their values are given in table 2. For KCl concentrations lower than 2.0 M the values of $(\partial\rho/\partial n_2)_\mu$ given in table 1 were inferred from both the sedimentation and diffusion coefficient measurements by means of eq. 7. The corrected values $s_{20,w}$ and $D_{20,w}$ of the sedimentation and diffusion coefficients were calculated according to

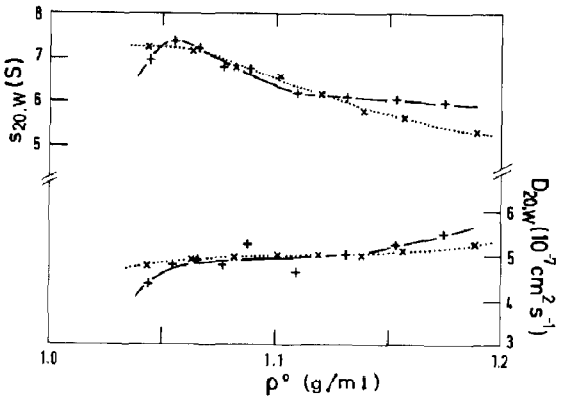

Fig. 2. Corrected sedimentation and diffusion coefficients of hMDHase particles.

Table 2

Sedimentation coefficient ($s_{20,sol}$) and diffusion coefficient ($D_{20,sol}$) of hMDHase in KCl of different concentrations (C_3) at 20 °C $s_{20,w}$, corresponding values corrected according to eqs. 4 and 6; ϕ', the quantity on the right-hand side of eq. 5.

C_3 (mol/l)	η_{sol}/η_w	$s_{20,sol}$ (S)	$s_{20,w}$ (S)	$D_{20,sol}$ ($\times 10^{-7}$) (cm^2/s)	$D_{20,w}$ ($\times 10^{-7}$) (cm^2/s)	ϕ' (ml/g)
4.00	1.054	3.44	5.98	5.19	5.47	0.693
3.50	1.0256	4.01	6.07	5.09	5.22	0.672
3.00	1.0068	4.52	6.10	5.01	5.04	0.660
2.50	0.9920	5.08	6.21	4.66	4.62	0.626
2.00	0.9905	5.80	6.76	5.29	5.24	0.637
1.75	0.9875	6.06	6.79	4.84	4.78	0.603
1.50	0.9862	6.62	7.22	4.96	4.89	0.584
1.25	0.9873	6.90	7.36	4.86	4.80	0.571
1.00	0.9904	6.63	6.96	4.40	4.36	0.554

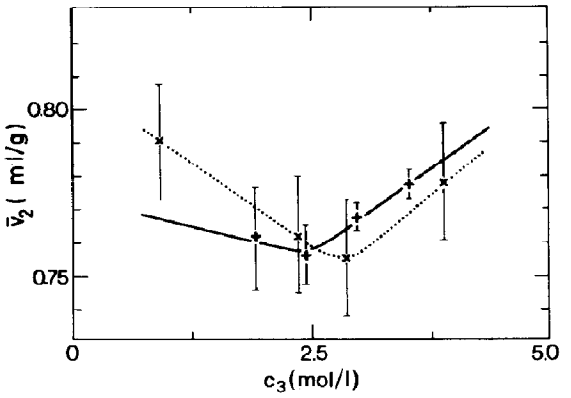

Fig. 3. Partial specific volume of hMDHase in KCl (+) and NaCl (×) solutions as a function of salt molarity (C_3) in the solvent.

eqs. 4 and 6, respectively. These are also listed in table 2. The quantity ϕ' needed to compute $s_{20,w}$ was deduced from the density increments by means of eq. 5. In fig. 2 both $s_{20,w}$ and $D_{20,w}$ are plotted vs. the mass density ρ^o of the solvent. For comparison, the corresponding results obtained previously [12] for NaCl buffers are also shown.

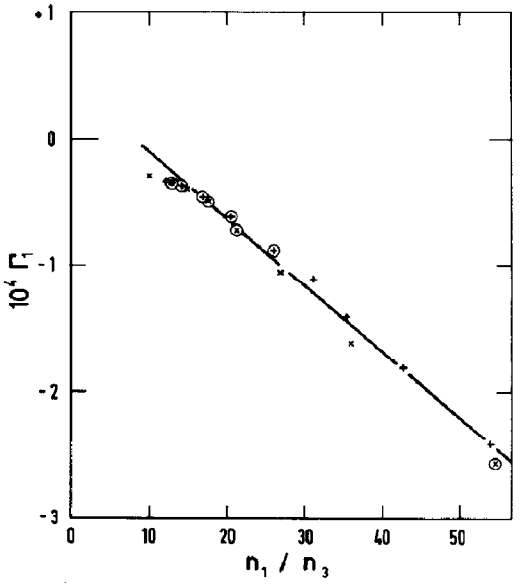

Fig. 4. Interaction parameter Γ_1 as a function of the salt concentration ratio (n_1/n_3): (+) KCl, (×) NaCl. Encircled symbols represent values inferred from both SANS and sedimentation measurements. The other points represent values deduced only from sedimentation measurements.

In fig. 1 all the values obtained for $(\partial\rho/\partial n_2)_\mu$ in KCl solvents are plotted vs. the solvent density ρ^o. The density increments are linear with ρ^o even for the higher salt concentrations investigated, with a slope $M_2V_{tot} = (1.55 \pm 0.1) \times 10^5$ ml per mol protein. This value is in good agreement with that deduced from SANS experiments. It is also more accurate because of the larger range of salt concentrations investigated. This is also true for the value of the intercept with the $\rho^o = 0$ axis, which corresponds to a molar mass $M_{tot} = 199 \pm 11 \times 10^3$ g/mol. Quite similar results have already been obtained for NaCl solutions [12] (fig. 1). Analysis of these results gives $m_2V_{tot} = (1.52 \pm 0.66) \times 10^5$ ml/mol protein and $M_{tot} = (193 \pm 9) \times 10^3$ g/mol.

For KCl concentrations varying from 2.0 to 3.5 M both sedimentation and SANS measurements are available. Values of the partial volume $\bar{v}_2$ and interaction parameter were calculated by solving eqs. 8 and 10, for each condition. For this purpose the density of water was assumed to be 0.9976 ± 0.0006 at $22.5 \pm 2.5\,^\circ$C; the respective values for the scattering length of water, KCl and hMDHase are -5.62×10^9, 10.7×10^9 and 14.8×10^9 cm/g.

The values calculated for $\bar{v}_2$ and Γ_1 are listed in table 1. In figs. 3 and 4, $\bar{v}_2$ and Γ_1 are plotted as functions of C_3 and the solvent molar ratio n_1/n_3, respectively.

The value of $(\partial\rho/\partial n_2)_\mu$ for 2.0 M KCl is about 7% lower than expected. This is very likely due to hMDHase denaturation. Of course, this discrepancy is also reflected in the values obtained for Γ_1 and $\bar{v}_2$. For instance, the linearly interpolated value of $\bar{v}_2$ is (0.761 ± 0.015) ml/g rather than (0.777 ± 0.013) ml/g.

When both sedimentation and SANS measurements were not available at a given KCl concentration the values of the interaction parameters were simply inferred from eq. 8 by taking the values of $\bar{v}_2$ listed in table 1. These values were extrapolated from the available data by means of the full curve drawn in fig. 3.

Similar data for NaCl solutions of hMDHase are also shown in figs. 3 and 4. They were calculated from the experimental values reported previously [10]. For both salts $\bar{v}_2$ appears to have a

Table 3

Radius of gyration (R_g) of hMDHase in solutions containing KCl at different concentrations (C_3)

x_2 is the scattering fraction of hMDHase.

C_3 (mol/l)	x_2	R_g (Å)
3.8	$0.89 \pm^{0.09}_{0.05}$	29.3 ± 0.3
3.5	$0.88 \pm^{0.09}_{0.05}$	29.5 ± 0.2
3.0	$0.86 \pm^{0.09}_{0.05}$	30.6 ± 0.32
2.5	$0.84 \pm^{0.08}_{0.05}$	30.1 ± 0.3
2.0	$0.82 \pm^{0.08}_{0.05}$	30.0 ± 0.5
1.5	$0.81 \pm^{0.08}_{0.05}$	30.8 ± 0.5

minimum for concentrations close to 2.5 M, but this is not outside experimental error and $\bar{v}_2$ could be considered constant and the same for both salts in the ranges studied. Within experimental uncertainties the molar interaction parameters are identical for both salts (fig. 4).

4.2. Particle structure

The values obtained for the radii of gyration of the different particle contrasts are listed in table 3. They are quite similar to those obtained from SANS experiments with solvents containing NaCl [10]. Two different large-angle scattering curves obtained for hMDHase in KCl solutions are shown in fig. 5. These curves are normalized to the forward scattering intensity $I(0)$. For the first one, corresponding to the larger range of q values, the solvent was heavy water containing 3.5 M KCl. In this case labile hydrogen atoms of hMDHase were replaced by deuterium. As for solvents containing NaCl [10] the forward scattering intensity indicates that about 80% of the hMDHase hydrogen atoms were exchanged. The radius of gyration of the particle contrast is found to be $R_g = (29.5 \pm$

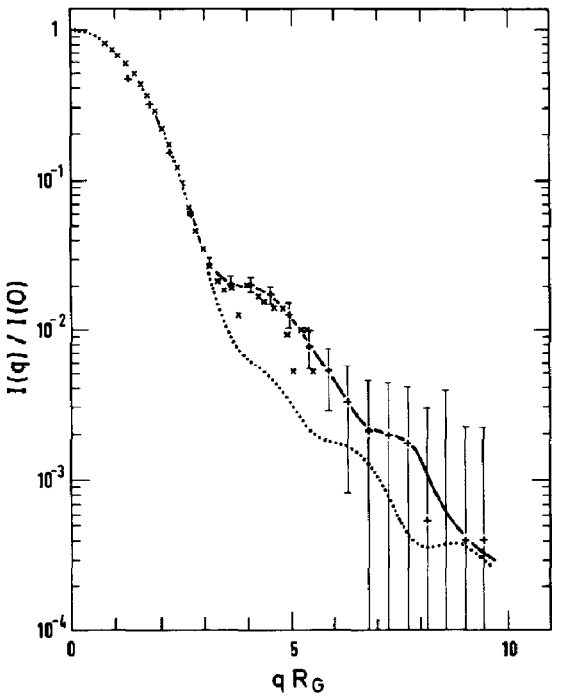

Fig. 5. Normalized neutron scattering intensity $I(q)/I(0)$ as a function of qR_g for hMDHase in KCl solutions: (+) 3.5 M KCl in ^2H_2O, (×) 3.8 M KCl in H_2O. (·····) Scattering curve of an oblate spheroid with an axial ratio of 0.6.

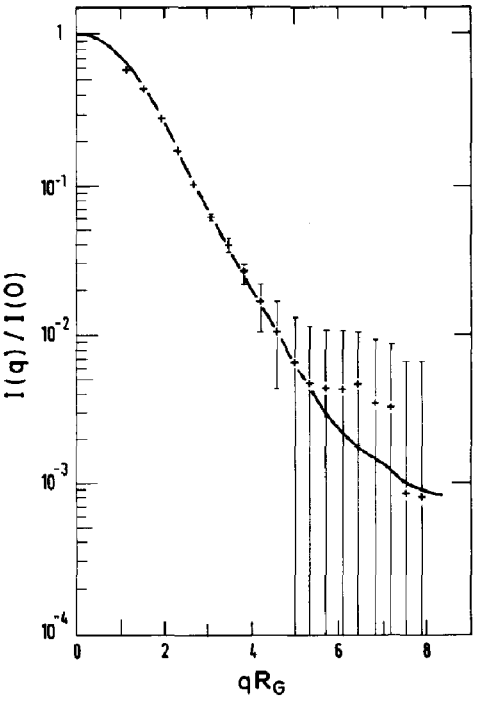

Fig. 6. Normalized neutron scattering intensity $I(q)/I(0)$ as a function of qR_g for mMDHase in a solvent containing ^2H_2O and 1.0 M KCl. The continuous curve represents the scattering curve of an oblate spheroid with an axial ratio of 0.4.

0.5) Å. For the other scattering curve the solvent was light water containing 3.8 M KCl. The radius of gyration of the hMDHase particle contrast is found to be $R_g = (29.3 \pm 0.3)$ Å. An arbitrary background adjustment was made to the curve by subtracting a constant from the experimental data. This correction is less than 30% of the statistical error in $I(q)$ for the larger values of q. The two small and sharp secondary minima are not significant. The two scattering curves in fig. 5 are similar. They are also similar to those obtained in NaCl buffers by both SANS and SAXS [10]. The dotted curve in fig. 5 represents the scattering curve of an oblate ellipsoid with an axial ratio of 0.6 and a constant scattering length density. As already mentioned by Reich et al. [22], for $qR_g < 3$, the particle is approximated well by an oblate or a prolate spheroid with an axial ratio of about 0.6 or 1.7, respectively.

Fig. 6 depicts the large-angle scattering curve of mMDHase in heavy water and 1.0 M KCl. The continuous curve corresponds to an oblate spheroid with an axial ratio of 0.4 and a radius of gyration of (24.6 ± 0.5) Å. The semi-axes of the spheroid are (37.6 ± 0.5) and (15.0 ± 0.6) Å. Within the experimental uncertainties this simple model correctly describes the data. The radius of gyration was also directly determined from the intensity scattered at lower scattering angles. In this case the solvent was light water with the same concentration of KCl. The radius of gyration was found to be (24.7 ± 0.3) Å in agreement with the value inferred from the ellipsoid model.

5. Discussion

For salt concentrations lower or equal to about 3.0 M, the density increment, scattering length density increment and interaction parameter are found to vary linearly with the mass density, scattering length density and the reciprocal of the relative salt concentration, respectively. This shows that neither the total volume V_{tot}, nor the total molar mass M_{tot} of the particle or the numbers of water and salt molecules associated with it vary with the solvent density in that range of salt concentrations. The values of M_{tot}, V_{tot} and L_{tot} given in table 4 result from the analysis of the experimental results given in section 4. Within experimental uncertainties they are the same irrespective of the salt. Solving the expression relating M_{tot} to N_1 and N_3 leads to the values of N_1 and N_3 listed in table 4. In either KCl or NaCl buffers, each hMDHase molecule is found to be associated with (4100 ± 460) water molecules and (520 ± 60) salt molecules. The values of the corresponding exclusion parameters B_1 and B_3 are also given.

From the values of N_1 and N_3 given in table 4 and the data of Wolf et al. [23], it can be inferred that the solvent associated with the enzyme has a constant KCl concentration of about 5.8 M, namely, well above saturation. For NaCl solutions the corresponding value is 6.1 M.

As far as the interaction parameters are concerned fig. 4 shows that Γ_1 has the same value for both salts. For salt concentrations lower than about 3.0 M Γ_1 varies linearly with n_1/n_3. According to eq. 13 the slope of the straight line and its intercept with the $n_1 = 0$ axis give the values of N_3 and N_1, respectively. They are found to be the same as those previously obtained and listed in table 4.

The first part of this section demonstrated that the invariant particle picture [10,20] describes the experimental results in a self-consistent way for salt concentrations lower than about 3.0 M. How-

Table 4

Parameters of the hMDHase particle in solvents containing less than 3.5 M salt

hMDHase	M_{tot} (kg/mol)	V_{tot} (ml/g)	L_{tot} ($\times 10^{15}$) (cm/mol)	N_1 (mol/mol)	N_3 (mol/mol)	B_1 (g/g)	B_3 (g/g)
In KCl solutions	199 ± 11	1.79 ± 0.11	$1.29 \pm \frac{0.06}{0.12}$	4080 ± 440	520 ± 60	0.84 ± 0.10	0.44 ± 0.06
In NaCl solutions	193 ± 9	1.74 ± 0.08	$1.28 \pm \frac{0.06}{0.21}$	4160 ± 400	530 ± 50	0.86 ± 0.09	0.36 ± 0.04

ever, the results displayed in figs. 1, 2 and 4 indicate that this may not be true for higher salt concentrations. Whereas the mass density increment is linear with solvent density, this is not so for the neutron scattering density increments at the higher salt concentrations for either NaCl or KCl solvents. Furthermore, this effect is reproducible and the NaCl and KCl data points fall on the same curve. The contradiction between the neutron scattering and mass density data is only an apparent one. The complementarity of SANS and mass density data arises from the fact that they have different sensitivity to the various contributions to the respective density increments [10]. Effects leading to non-linearity for SANS might be negligible for mass density. For this reason, before applying the invariant volume hypothesis to the entire salt range, both the mass density and neutron scattering density increments should be linear. If we assume that the deviations from linearity are real, the mass density and neutron scattering data taken together from solvents with the highest salt concentrations can only be explained by assuming that the particle composition varies with the solvent density. It is then found that both the numbers of water and salt molecules associated with one hMDHase molecule decrease with increasing salt concentrations. A good fit to both the mass density and neutron scattering data is obtained in the 3.5–4 M salt range with N_1 decreasing gradually to 1000 mol water per mol protein and N_3 to 350 mol salt per mol protein. These values lead to negligible deviations from linearity for the mass density data, but not for those of neutron scattering.

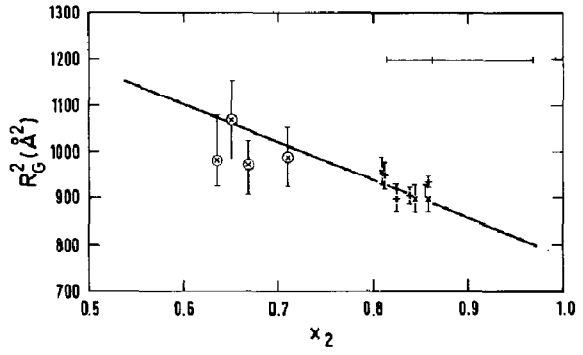

Fig. 7. Squared radius of gyration R_g^2 of hMDHase particles as a function of the hMDHase scattering fraction x_2. (+) KCl solutions, (×) NaCl solutions. Encircled symbols are inferred from SAXS experiments [22] while the other points are deduced from SANS measurements. The horizontal bar represents the typical systematic error in x for SANS results. Salt concentrations never exceeded 3.0 M.

In fig. 7 the radius of gyration R_g of the particle contrast is plotted vs. the scattering fraction x_2 of hMDHase for KCl concentrations lower than 3.5 M. Also shown are the data derived from SANS [10] and SAXS [22] measurements for solvents containing less than 3.5 M NaCl. For both salts R_g values are similar. They decrease slightly with increasing values of x_2. Because the scattering fraction of the enzyme varies only weakly with the salt concentration in the solvent a quantitative analysis of the above results is rather difficult. Quite generally the centers of excess scattering of the particle components may be different. However, because of the similarity of the scattering curves obtained for different salt conditions, it can reasonably be assumed that these centers coincide [10]. Then according to eqs. 17 and 18, the experimental data shown in fig. 7 give $R_{g2} = (27.9 \pm 1.8/1.4)$ Å for hMDHase alone ($x_2 = 1$), $R_{gs} = (40.0 \pm 4.0/5.9)$ Å for the associated solvent alone ($x_2 = 0$) and $R_g = (34.5 \pm 1.8/2.6)$ Å for the whole particle if homogeneous ($x_2 = 0.5$). These results are not very accurate but they can be regarded as reliable estimates within the given uncertainties. They show that the water and salt associated with hMDHase lie towards the particle periphery.

At very low resolution, the particle can be modelled by an oblate spheroid with an axial ratio of 0.6. Its volume is 255 nm^3 (calculated from V_{tot}). This particle would have a radius of gyration of 32 Å if it were homogeneous. Furthermore, a globular protein shaped as an oblate spheroid with axial ratio 0.60 ± 0.05 would have a radius of gyration $R_{g2} = (24.1 \pm 0.7)$ Å. These calculated values for R_g and R_{g2} are lower than those observed. This shows that the particle is not homogeneous and that part of the protein component is at larger radii than it would be for a globular protein. These results are in agreement with the model discussed by Zaccai et al. [10]. Under non-denaturating salt conditions, hMDHase in solution

can be regarded as having a central compact core with protruding parts in contact with the associated water and salt. This model also explains the relatively high first shoulder of the scattering curves in fig. 5 [10]. Such a shoulder is absent from the scattering curve of the non-halophilic mMDHase which can be modelled well as a globular enzyme shaped like an oblate spheroid.

In conclusion, hMDHase differs from non-halophilic mMDHase in a number of structural features probably associated with its halophilic character. It is a larger molecule and richer in acidic but poorer in basic amino acids [13]. It has a low-resolution structure with an involuted surface or protuberances in interaction with relative large numbers of water and salt molecules. These numbers are constant, regardless of whether the solvent contains NaCl or KCl, which argues in favour of non-specific interactions between protein sites and the monovalent salts. As has been shown by denaturation studies in low salt [11,24] these exceptional interactions disappear when the quaternary structure of the enzyme is lost.

Acknowledgement

P.C. and G.Z. are grateful to Mme. M. Lambert for initiating and supporting their collaboration.

References

1 B. Schobert and J.K. Lanyi, J. Biol. Chem. 257 (1982) 10306.
2 M.M. Werber, M. Mevarech, W. Leicht and H. Eisenberg, in: Energetics and structure of halophilic microorganisms, eds. S.R. Caplan and M. Ginzburg (Elsevier/North-Holland, Amsterdam, 1978) p. 427.
3 R. Jaenicke, Annu. Rev. Biophys. Bioeng. 10 (1981) 1.
4 C.R. Woese, and G.J. Olsen, Syst. Appl. Microbiol. 7 (1986) 161.
5 C.R. Woese and R.S. Wolfe, The bacteria, vol. VIII (Academic Press, Orlando, FL, 1985).
6 D.J. Kushner, in: The bacteria, vol. VIII, eds. C.R. Woese and R.S. Wolfe (Academic Press, Orlando, FL, 1985) p. 171.
7 B. Wilkansky (Elazari-Volcani), Nature 138 (1936) 467.
8 M. Ginzburg, L. Sachs and B.Z. Ginzburg, J. Gen. Physiol. 55 (1970) 187.
9 H. Eisenberg, Biological macromolecules and polyelectrolytes in solution (Clarendon Press, Oxford, 1976).
10 G. Zaccai, E. Wachtel and H. Eisenberg, J. Mol. Biol. 190 (1986) 97.
11 S. Pundak and H. Eisenberg, Eur. J. Biochem. 118 (1981) 463.
12 S. Pundak, H. Aloni and H. Eisenberg, Eur. J. Biochem. 118 (1981) 471.
13 M. Mevarech, H. Eisenberg and E. Neumann, Biochemistry 16 (1977) 3781.
14 K. Ibel, J. Appl. Crystallogr. 9 (1976) 630.
15 J.P. Cotton, L.L.B. Internal Report no. 758 (1984).
16 B. Jacrot and G. Zaccai, Biopolymers 20 (1981) 2413.
17 A. Guinier and G. Fournet, Small angle scattering of X-rays, (Wiley, New Yor, 1955).
18 E.F. Casassa and H. Eisenberg, Adv. Protein Chem. 19 (1964) 287.
19 H. Eisenberg, Q. Rev. Biophys. 14 (1981) 141.
20 V. Luzzati and A. Tardieu, Annu. Rev. Biophys. Bioeng. 9 (1984) 1.
21 P.B. Moore, D.M. Engelman and B.P. Schoenborn, J. Mol. Biol. 91 (1973) 101.
22 M.H. Reich, Z. Kam and H. Eisenberg, Biochemistry 21 (1982) 5189.
23 A.V. Wolf, M.G. Brown and P.G. Prentiss, in: C.R.C. handbook of chemistry and physics, 57th edn., ed. R.C. Weast (C.R.C. Press, Cleveland) D-218.
24 G. Zaccai, G. Bunick and H. Eisenberg, J. Mol. Biol. 92 (1986) 155.